United Nations Educational, Scientific and Cultural Organization
GRÓ GTP Geothermal Training Programme Under the auspices of UNESCO

GRÓ GTP, Grensásvegur 9,
IS-108 Reykjavík, Iceland

Reports 2021
Number 19

# GEOCHEMICAL CHARACTERISTICS OF SAN FRANCISCO LIBRE GEOTHERMAL RESOURCE IN NICARAGUA

**Rebeca Ortiz López**
Ministry of Energy and Mines -MEM
Costado este del Parque Las Palmas,Managua
NICARAGUA
*Chemestry0611@gmail.com*

## ABSTRACT

Data from geochemical exploration of the San Francisco Libre geothermal area in Nicaragua are presented. Out of about 30 water samples collected, six samples were selected for more detailed processing. The chemical composition of these fluids was analysed by standard methods. The ternary Cl-$SO_4$-$HCO_3$ diagram was used to classify the geothermal fluids with respect to major anion composition and the ternary Na-K-Mg diagram was used to classify waters according to the state of equilibrium at given temperatures. The geothermal fluids of San Francisco Libre are of bicarbonate-sulphate type, but a more chloride-rich fluid was also observed. The WATCH software was used to interpret the equilibrium state of the system and to predict the temperature of the geothermal resource. The study confirms the presence of a low-salinity geothermal system with a temperature of 75-85°C, with Na/K and chalcedony geothermometers in good agreement with measured temperatures. Another, more saline geothermal system is inferred with a chalcedony temperature of 115-120°C whereas the measured temperature is only about 35°C.

## 1. INTRODUCTION

Nicaragua has abundant geothermal resources including both high and low temperature areas along the active volcano range Los Maribios, which runs along the country's Pacific coast (Figure 1). Maribios volcanic range consists of active volcanoes, some lagoons, volcanic structures, and extensive areas of hydrothermal activity, denoting the presence of a magmatic heat source at depth. Interaction between the Cocos, Nazca, and Caribe Plates with the North and South American Plates results in a complex structural pattern of the terrestrial crust in Central America. Since the Jurassic, multiple geotectonic events have occurred. Today, the triangular Cocos Plate borders the Pacific Plate in the west, the Nazca Plate in the south, the North American Plate in the north, and the Caribbean Plate in the northeast through Central America in the subduction zone along the Mesoamerican Trench (Kristinsson and Ruíz, 2011). The formation of the Nicaraguan crust is the result of the interaction of several plates which began with the split of Pangea approximately 250 Ma (Burke et al., 1984) followed by the collision of the Farallón Plate with the Proto-Caribbean crust (Arch of primitive Toledo islands) which occurred between the Albian and Santonian periods (Seyfried, 1991). In this paper, I show the results from analysis of data obtained from the San Francisco Libre geothermal area in Nicaragua in 2013, taken from the MEM data base unpublished data.

The research area for this study, the San Francisco Libre geothermal area, is roughly 60 km$^2$ in size, most of which is on dry land and just around 5 km$^2$ under the surface of Lake Xolotlán. The region comprises the San Francisco metropolitan center as well as the communities of El Porvenir, Loma San Francisco, San Luis, Los Genizaros, El Rosario 1 and 2, Bella Vista, and La Paz (Kristinsson and Ruíz, 2011). The "José de la Cruz Mena" Medical Center for Hydrotherapy and Fangology is in San Francisco Libre, just a kilometer and a half from the urban area of San Francisco, which is the only place in Nicaragua specialized in curing skin diseases by means of application of volcanic mud and thermal water, coming from several local thermal sources (Kristinsson and Ruíz, 2011). In Nicaragua, natural medicine for the treatment of diseases has been used since ancient times.

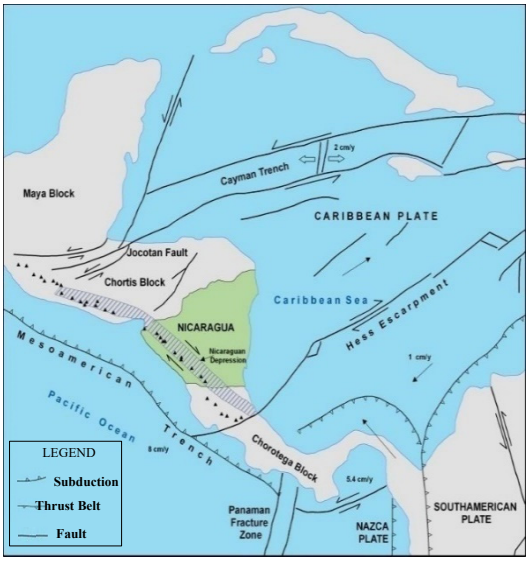


FIGURE 1: Tectonic scheme of the Central American Region (Kristinsson and Ruíz, 2011)

## 2. STUDY AREA

### 2.1 Study location

The San Francisco Libre administrative area has a total area of 756 km$^2$ and is home to 33 communities organized into four regions: San Roque, Telpochapa, Laurel Galán, and San Francisco (ENACAL, 2021). San Francisco has an area of roughly 72 km$^2$ and is located around 80 km north of Managua along the north coast of Lake Xolotlán (Lake Managua). It has a population of 10,503 people, 3,080 of whom live in the urban area and a rural population of 7,423 inhabitants (ENACAL, 2021).


FIGURE 2: San Francisco Libre study area (black box) location map (Kristinsson and Ruíz, 2011)

### 2.2 San Francisco libre geology

San Francisco Libre's lithology is characterized by ignimbrites and basaltic lavas from the Pliocene Upper Coyol Group as well as alluvial and lake sediments such as Quaternary deposit clays, which cover primarily Tertiary rocks and most of the research area. Well-fractured basalts on the surface and perhaps beneath well-altered ignimbrites that are difficult to identify can be encountered east of San Francisco Libre area (Figure 2). A little farther south, there are some fragmentary altered rock outcrops that run-in northeast-southwest direction, parallel to the lineament that forms the northeast boundary of the Nicaraguan depression through which hot springs flow (Kristinsson and Ruíz, 2011). To the southeast of the zone, well-weathered ignimbrites outcrop in the upper and underlying layers of ash, most likely from the Momotombo volcano's eruptive activities, with intercalations of alluvial deposits potentially of well-altered whitish ignimbrites of different granulometry both in the upper and bottom layers.

The regional lineament is parallel to the Nicaraguan depression which exhibits significant tectonic activity covered by Quaternary deposits. Cracks with a North-South direction can be observed in some areas of the outcrop, in some cases filled with gypsum ($CaSO_4 \cdot H_2O$) deposits. Faults and fractures with a Northwest - Southeast orientation are more visible in the research region's northern part (Kristinsson and Ruíz, 2011).

### 2.3 Geothermal Manifestations

Geothermal manifestations in the study area are found on the northeast coast of Lake Xolotlán (see Figure 3), southeast of San Francisco Libre, and near the San Luis farm.

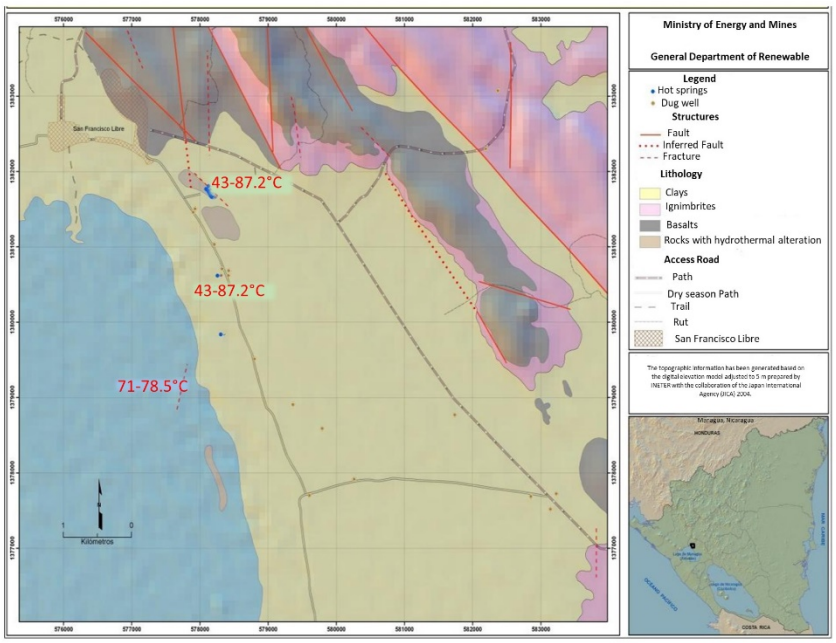


FIGURE 3: Geological map of the San Francisco Libre area (Kristinsson and Ruíz, 2011)

The largest manifestation is near the Medical Center where it is being used to treat dermatological conditions. It consists of numerous small hot springs within a system of fractures that have a N50E direction. The total estimated flow from the springs is 0.5 to 1.5 L/s (Kristinsson and Ruíz, 2011). Small mounds may be seen on the lake's coast. Hydrothermal alteration seen as several white islets that are positioned parallel to these mounds (see Figures 4, 5 and 6). These islets are calcite (Kristinsson and Ruíz, 2011) and are most likely Tertiary in age.

FIGURE 4: Thermal sources in the Medical Center (Kristinsson and Ruíz, 2011)

FIGURE 5: Small white Mounds (Kristinsson and Ruíz, 2011)

FIGURE 6: Xolotlán Lake rock alteration (Kristinsson and Ruíz, 2011)

Another system of fractures with NNE-SSW orientation extends from the northern half of the study area. These fractures meet at the medical center where they were discovered outflow of hot water with temperatures ranging from 71 to 78.5°C and an approximate flow rate of 0.3 L/s. The geological map corresponding to Figure 3 shows the direction of the fracture (Kristinsson and Ruíz, 2011).

## 3. METHODS

### 3.1 Sampling and analysis

In April 2013, the Geochemical Laboratory of the Ministry of Energy and Mines of Nicaragua collected a total of 30 water samples in the San Francisco geothermal exploration area (Figure 7). Temperature, pH, and electrical conductivity (EC) were measured on site with handheld meters with a Hach HQ40d multiparametric Probe (calibrated prior to sampling). The samples were filtered through a 0.45 µm filter and analyzed using the following methods: $CO_3^{2-}$ and $HCO_3^-$ analysis by volumetric titration, cation analysis (Na, K, Ca, Mg, Fe, Li, Rb, As) by atomic absorption spectrophotometry (Varian EAA 240FS) with Flame technique, $SiO_2$ analysis by UV-VIS spectrophotometry (Varian Cary 50), using the ammonium molybdate method, B analysis by UV-VIS spectrophotometry using the Azomethine-H method, Cl analysis by argentometric titration and $SO_4$ analysis either by an indirect spectrophotometric method with barium chromate and bromophenol blue or by ion chromatography (for $SO_4$ less than 20 ppm). All methods are described by Pang and Ármannsson (2006).

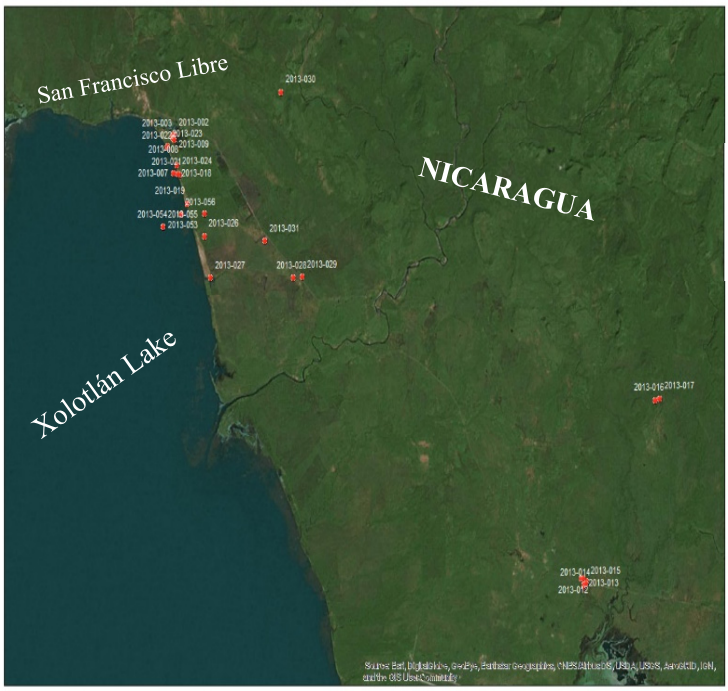


FIGURE 7: Geographical location map for the San Francisco Libre samples (red points)

### 3.2 Water classification

A common first step in classification of geothermal waters is to group waters in terms of the dominant anions and to look at the processes that lead to the formation of those waters. This is done by using the classification scheme and ternary diagram of Giggenbach (1988) which assumes a volcanic high-temperature geothermal system. For low-temperature geothermal waters in fracture-controlled settings, the diagram is still useful, but generally the water composition is controlled by other processes than those described by Giggenbach (1988), most commonly only water-rock interaction.

*Chloride waters*

This kind of water, sometimes known as "alkali-chloride" or "neutral-chloride," is typical of the deep geothermal fluid found in most high-temperature systems. Hot, large-flow springs with high Cl content are supplied more directly from the deep reservoir, indicating permeable zones within the field. However, because local topography can have a considerable influence on hydrology, these locations may not necessarily overlie the primary upflow zone. Chloride is the main anion with concentrations ranging from hundreds of mg/kg to more than 10,000 mg/kg. At the temperature of measurement, the pH is usually slightly acidic or alkaline, i.e. near-neutral (Nicholson, 1993).

*Sulphate waters*

According to Nicholson (1993), sulphate-waters in high-temperature settings are generally produced by the condensation of geothermal gases into near-surface oxygen-rich groundwater. The gases, together

with steam and other volatiles were first dissolved in the deep fluid, then separated from it after boiling at depth. They are often located at high topographic levels above the water table and above boiling zones. Although sulphate waters are often found at the surface (< 100 m), they can reach deep into the geothermal system via faults. The main anion is sulphate, which is produced by oxidizing hydrogen sulphide.

$$H_2S_{(aq)} + 2\ O_{2(aq)} = 2\ H^+_{(aq)} + SO_4^{2-}{}_{(aq)} \quad (1)$$

This reaction produces protons, creating acid waters. The oxidation of hydrogen sulphide to sulphate ions results in a pH of around 2.8. A magmatic gas contribution is expected if the water is substantially more acidic than this (pH < 2.0).
In a low-temperature setting, a high sulphate concentration generally reflects a sulphate-rich mineralogy.

*Bicarbonate waters*
These waters, which include those termed $CO_2$-rich fluids and neutral bicarbonate-sulphate waters, are the product of steam and gas condensation into poorly oxygenated sub-surface groundwaters or if the concentration of $H_2S$ in the steam is low. Such fluids can occur in an umbrella-shaped perched condensate zone overlying the geothermal system and are common on the margins of fields. Bicarbonate waters are found in non-volcanogenic, high-temperature systems (Nicholson, 1993), but also in low-temperature systems.

The Cl-$SO_4$-$HCO_3$ ternary diagram is used to categorize geothermal fluids according to their primary anion concentrations (Giggenbach, 1988). It aids in the identification of young unstable waters and provides an early indication of mixing linkages or regional groups. A data point's location in this plot is determined by first computing the total of the concentrations C (mg/kg) of all the species involved:

$$\sum anion = C_{Cl} + C_{SO4} + C_{HCO3} \quad (2)$$

The following step is to calculate the percentage of each ingredient using the following equation:

$$\%Cl = \frac{100C_{Cl}}{\sum anion}; \%SO_4 = \frac{100C_{SO_4}}{\sum anion}; \%HCO_3 = \frac{100C_{HCO_3}}{\sum anion} \quad (3)$$

This plot demonstrates the compositional ranges for the many types of fluids found in geothermal areas, such those described above and combinations and variations thereof.
The Na-K-Mg equilibrium ternary diagram is used to categorize water as fully equilibrated, somewhat equilibrated, or immature. It can anticipate the equilibrium temperature as well as the appropriateness of using thermal waters as ionic solute geothermometers. It is based on the temperature dependence of the entire equilibrium composition of potassium and sodium minerals which emerges following the isochemical recrystallization of ordinary crustal rock under geothermal circumstances (Giggenbach, 1988). The triangle diagrams are used due to the temperature dependency of the three reactions:

$$K\text{-}feldspar + Na^+ = Na\text{-}feldspar + K^+ \quad (4)$$

$$0.8\ muscovite + 0.2\ clinochlore + 5.4\ silica + 2\ Na^+ = 2\ albite + 0.8\ K\text{-}feldspar + 1.6\ water + Mg^{2+} \quad (5)$$

$$0.8\ muscovite + 0.2\ clinochlore + 5.4\ silica + 2\ K^+ = 2\ albite + 2.8\ K\text{-}feldspar + 1.6\ water + Mg^{2+} \quad (6)$$

The Na-K-Mg triangular diagram indicates that the water-rock equilibrium has been reached if the data point plots on the full equilibrium line. The water is immature if the data point is located below the "immature water curve," indicating an initial dissolution of minerals before the equilibrium reaction takes place. In the latter instance, geoindicators cannot be employed. The field of partial equilibrium is located between those two curves and denotes either a mineral that has dissolved, equilibrium reactions

that have begun but equilibrium has not yet been reached, or a mixture of a water that has reached equilibrium (e.g., geothermal water) and a dilute unequilibrated water (e.g., cold groundwater). Temperatures measured using geothermometers are frequently inaccurate.
The Na-K-Mg triangular diagram is constructed in a similar manner as the Cl-$SO_4$-$HCO_3$ ternary, but the concentrations are scaled to compensate for the differences in the ionic charges and typical concentrations of the three components. Therefore, the cation sum is defined as follows:

$$S = C_{Na^+}/1000 + C_{K^+}/100 + \sqrt{C_{Mg^{2+}}} \quad (7)$$

The following step is to calculate the percentage of each ingredient using the following equation:

$$\%Na = \frac{100C_{Na}}{1000\sum anion}; \%K = \frac{100C_K}{100\sum anion}; \%Mg = \frac{100\sqrt{C_{Mg^{2+}}}}{\sum anion} \quad (8)$$

### 3.3 Geothermometry

Geothermometry is employed during the exploration phase to estimate subsurface temperatures (Arnórsson, 2000). Geothermometers are a crucial tool to determine the temperature in a geothermal reservoir and according to Arnórsson (2000) are divided into three types:

1. Water or solute geothermometers,
2. Steam or gas geothermometers, and
3. Isotope geothermometers.

The essential use of chemical and isotopic geothermometers all through geothermal exploration is to estimate reservoir temperatures below the zone of cooling. When geothermometers are used to measure subterranean or aquifer temperatures, the assumption is always made that temperature dependent chemical or isotopic equilibria exist in the source aquifer (Arnórsson, 2000). As all the data samples collected for this study are from water samples, only water geothermometers will be discussed below.

*Water Geothermometers*
According to Nicholson (1993), geothermometers enable the temperature of the reservoir fluid to be estimated. They are therefore valuable tools in the evaluation of new fields and in monitoring the hydrology of systems in production. Solute geothermometers are based on temperature dependent mineral-fluid equilibria and their successful application relies on five basic assumptions (Fournier et al., 1974; Truesdell, 1976; White, 1970):

1. The concentration of the elements or species to be used in the geothermometer is controlled only by a temperature dependent mineral fluid reaction.
2. There is an abundance of the minerals and/or dissolved species in the rock fluid system for the reaction to occur readily.
3. The reaction attains equilibrium in the reservoir.
4. There is rapid flow to the surface with no re-equilibration after the fluid leaves the reservoir, i.e., no near surface reactions.
5. There is no mixing or dilution of the deep fluid (this assumption can be circumvented if the extent of dilution/mixing can be evaluated).

Like any tool, geothermometers must be used correctly:

Hot (ideally boiling) springs with a high chloride concentration and a good flow rate (> 1 L/s) provide the most reliable results. Their waters will have risen to the surface rapidly, with minimal opportunity for rock water reactions or re-equilibration to occur. In the reservoir host rock, there is an abundance of

the mineral involved in the geothermometry reaction.

The reaction must be rapid enough to establish equilibrium in the reservoir but, to ensure the reservoir composition is retained in the discharge water, it should not be so rapid that it re-equilibrates as the fluid migrates to the surface.

The silica (quartz and chalcedony), Na/K, and Na-K-Ca water geothermometers are the most important geothermometers. Others based on Na/Li, Li/Mg, K/Mg ratios, and Na-K-Mg correlations have also been developed (Arnórsson, 2000).

*Quartz geothermometers*
The quartz geothermometer, which is based on quartz solubility, is used to assess subsurface temperatures in hot spring systems. Quartz solubility is affected by pressure, temperature, and salinity. Quartz geothermometers perform well in systems with subsurface temperatures ranging from 120ºC to 300°C but calibrations exist for higher temperatures (Arnórsson, 2000). The fundamental process for silica mineral dissolution is:

$$SiO_{2(s)} + 2\ H_2O = H_4SiO_{4(aq)} \quad (9)$$

Taking the enthalpy of such reactions to be constant is a fair assumption for many silicate-water reactions, at least up to roughly 250°C. This equation is especially useful when experimental or drillhole data are used to calibrate geothermometers that only covers a narrow temperature range and must be extrapolated to lower or higher temperatures. For the quartz geothermometer, the following equation was utilized in this investigation.

Quartz – no steam loss (Fournier, 1977):

$$t°C = \frac{1309}{5.19 - logSiO_2} - 273.15 \quad (10)$$

*Chalcedony geothermometers*
This geothermometer is based on chalcedony's solubility. Fournier (1991) proposed that the use of silica geothermometers at temperatures below 180°C is ambiguous since chalcedony appears to govern dissolved silica in some areas and quartz in others. Chalcedony is an extremely fine-grained variant of quartz that is most likely not a distinct mineral but a combination of quartz and moganite that will completely transform to quartz over time (Gíslason et al., 1997).

Temperature, time, and fluid composition all influence the many crystalline forms of silica. As a result, in older systems where water has been in touch with rock at a particular temperature for a long period, quartz may regulate dissolved silica at temperatures as low as 100°C. At temperatures up to 180°C, chalcedony may regulate dissolved silica in younger systems. The following equation for chalcedony geothermometry was utilized in this investigation.

Chalcedony – no steam loss (Fournier, 1977):

$$t°C = \frac{1032}{4.69 - \log SiO_2} - 273.15 \quad (11)$$

*Na-K geothermometer*
Ion exchange processes with temperature-dependent equilibrium constants underpin cation geothermometers. The exchange of $Na^+$ and $K^+$ between co-existing alkali feldspars is a good example:

$$NaAlSi_3O_8(s) + K^+(aq) = KAlSi_3O_8(s) + Na^+(aq) \quad (12)$$

For this reaction, the equilibrium constant $K_{eq}$ is:

$$K_{eq} = \frac{(KAlSi_3O_8)(Na^+)}{(NaAlSi_3O_8)(K^+)} \quad (13)$$

If the activities of the solid reactants are assumed to be unity and the activity of the dissolved species is approximately equal to their molal concentrations, the equation is simplified to:

$$K_{eq} = \frac{[Na^+]}{[K^+]} \quad (14)$$

Several writers proposed empirical Na/K geothermometers based on tests with varying findings working with different minerals. At low temperatures, basaltic minerals typically yield low values (Arnórsson et al., 1983) whereas andesitic minerals offer high values (Giggenbach, 1988). They converge and produce identical results at high temperatures. In general, the Na/K ratio works well for calculating water temperatures over 200°C. In this paper, the formula utilized is based on empirical correlations reported by Arnórsson et al. (1983). Na and K concentrations are given in milligrams per kilogram (mg/kg):

*Na-K temperature (Arnórsson et al., 1983):*

$$t°C = \frac{933}{0.933 - log\frac{Na}{K}} - 273.15 \quad (15)$$

*Na-K-Ca geothermometer*

Fournier and Truesdell (1973) created the Na-K-Ca geothermometer for use in waters with high $Ca^{2+}$ concentrations which result in an abnormally high computed temperature for the Na/K geothermometer. The $Ca^{2+}$ participation in aluminium silicate processes was used to explain the connections between $Na^+$, $K^+$, and $Ca^{2+}$. The quantity of dissolved Na and K is thus regulated by the amount of dissolved Ca, even if the final amount of aqueous Ca could be mostly controlled by carbonate solubility and carbon dioxide (Nicholson, 1993).

$$t°C = \frac{1647}{log\left(\frac{Na}{K}\right) + \beta\left[log\left(\frac{\sqrt{Ca}}{Na}\right) + 2.06\right] + 2.47} - 273.15 \quad (16)$$

were

$$\beta = \frac{4}{3}\ for \frac{Ca^{\frac{1}{2}}}{Na} > 1\ and\ t < 100°C \quad (17)$$

$$\beta = \frac{1}{3}\ for \frac{Ca^{\frac{1}{2}}}{Na} < 1\ and\ t > 100°C \quad (18)$$

### 3.4 Mineral solution equilibrium

According to Arnórsson (2000), groundwater systems, such as a geothermal system, are defined by the movement of a fluid (water, steam, or a water-steam combination) through a body of rock. This water will chemically react with the rock, bringing the system closer to equilibrium as with any chemical reaction. The degree to which equilibrium is attained at each place in the system (local equilibrium) is determined by reaction rates and the rate of through-flowing water. The rate of reaction constantly increases as the temperature rises. It is a good rule of thumb to expect reaction speeds to rise two to three times for every 10°C increase in temperature. As a result, a 100°C rise increases reaction rates by $2^{10}$ to $3^{10}$, or 1000 to 60000 times. It is not unexpected, then, that rocks are often significantly altered in high temperature geothermal systems (T > 200°C), but minimal alteration is found in rocks near the Earth's surface if they have never been appreciably heated after creation.

The proximity of specific local chemical equilibria in a geothermal system is determined by: (1) the system temperature; (2) the rate of flows of matter between phases and aqueous species in the system; (3) the rate of flows of matter through the system; and (4) the amount of mass transfer required to achieve equilibrium.

Any chemical reaction's free Gibbs energy is provided by the equation:

$$\Delta G_r = \Delta G_r^0 + RTlnQ \tag{19}$$

Where $\Delta G_r^0$ is the standard Gibbs energy of reaction, $R$ is the gas constant, $T$ the temperature in kelvin and $Q$ is the reaction quotient. The equilibrium constant $K$ is related to the conventional Gibbs energy of reaction by the equation:

$$\Delta G_r^0 = -RTlnK \tag{20}$$

and thus, at equilibrium (where $\Delta G_r = 0$):

$$RTlnK = RTlnQ \tag{21}$$

or $K = Q$. If $K \neq Q$ and $\Delta G_r \neq 0$, there is no equilibrium.

The saturation indices SI for minerals in aqueous solutions at various temperatures were calculated as follows:

$$SI = log\frac{Q}{K} = logQ - logK \tag{22}$$

Comparison with the equation above shows that at equilibrium where $K = Q$, SI equals to 0. If SI < 0, the mineral has a tendency to dissolve, i.e., the solution is undersaturated with respect to the mineral, whereas if SI > 0, the solution is supersaturated, and the mineral will precipitate. If a solution is at equilibrium with several minerals at a particular temperature, the saturation index curves for those minerals will converges with SI = 0 at that temperature. The saturation indices (log(Q/K)) in this study were calculated with the WATCH program version 2.4 (Arnórsson and Bjarnason, 1993; Bjarnason, 2010) for the temperature range 50-120°C for the first group of samples (Medical center-Peña Blanca) and the range of 25 to 150°C for the sample that belongs to the second group.

### 3.5 Geochemical modelling

As an aqueous speciation software, the computer program WATCH (Arnórsson and Bjarnason, 1993) is a valuable tool for analyzing the chemical composition of geothermal fluids. It can also be used to compute various geothermometer temperatures. It was created to compute the aqueous speciation of geothermal reservoir fluids. The program's input is a component analysis of each phase (liquid, gas, steam) of the geothermal fluid at the surface including the water pH and temperature at which these values was measured, as well as the reference temperature for calculating the aqueous speciation. The quartz, chalcedony, and Na-K geothermometer temperatures are all calculated by the software. Most of the chemical components found in high quantities in geothermal fluids and/or rocks in geothermal systems are covered. WATCH determines the concentration and activity coefficient for each of the 69 aqueous species studied in the program, assuming homogeneous equilibrium in the solution.

## 4. RESULTS

All the samples from San Francisco Libre were taken from hot springs and wells, some of which were found abandoned. The sampling was executed during the dry season and the chemical analyses for the 30 samples of San Francisco Libre were completed in the geothermal laboratory of the Ministry of Energy and Mines of Nicaragua. The results are shown in tables in Appendix II.

The San Francisco Libre samples are divided into three groups. The first group is characterized by high temperature (> 75°C), minimum and maximum temperatures are 25°C and 85°C, respectively, as well as low chloride content and high silica content. The second group is characterized by low sampling temperatures, high chloride content and high silica content, also one of the samples from the second group has a high boron content. The total solids values for these samples range from 213 mg/L to 941 mg/L, the five samples with the highest sample temperature (> 75°C) are the following: 2013-004, 2013-005, 2013-006, 2013-053, and 2013-054, all from the Medical center or Pena Blanca.

To get an overview of the sample characteristics, the concentrations of sodium, magnesium, sulphate, silica, boron, temperature, and pH are plotted against chloride in Figure 8.

Through the observation of the binary plots, 3 groups of samples could be clearly identified, a group with low chloride content but high temperature > 75°C, a second group with high chloride content but low sampling temperature and a third group with high boron and magnesium content which could mean ground water with some mixing.

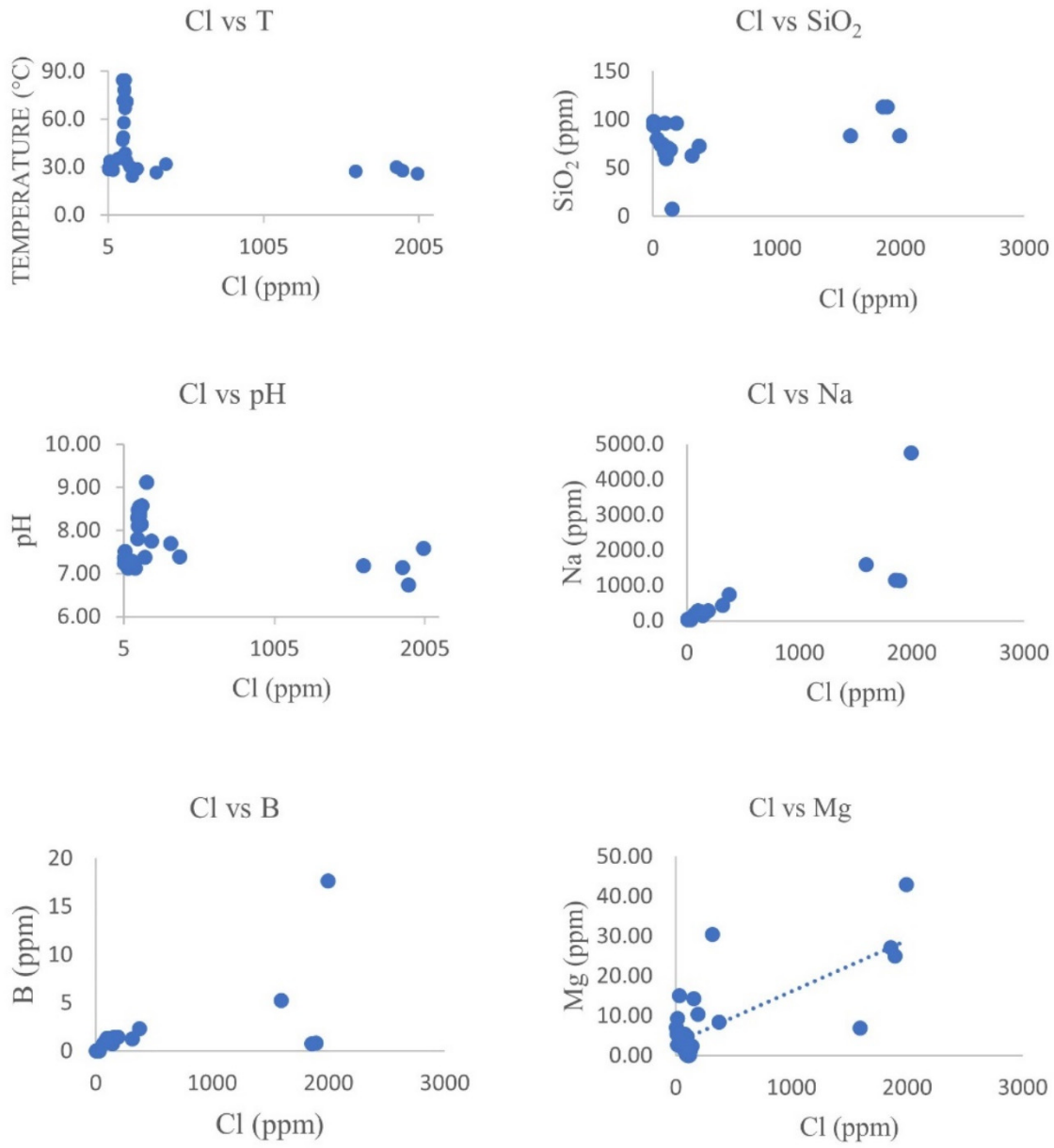


FIGURE 8: Binary plots for 30 water samples from San Francisco Libre, Nicaragua

### 4.1 Water classification

*Cl-SO4-HCO3 diagram*

The water samples from the San Francisco Libre area are plotted on the Cl-$SO_4$-$HCO_3$ ternary diagram (Powell and Cumming, 2010) in Figure 9. Most of the samples are systematically distributed in the sulphate and carbonate corners. Only 3 samples plot close to the chloride corner.

*Na-K-Mg diagram*

The Na-K-Mg triangular diagram indicates the equilibrium temperatures of minerals containing these elements and was used to identify the equilibrium between the geothermal fluids and rock and to determine the reservoir temperature. Most of the hot spring samples plot on the full range to ground water to geothermal water in equilibrium with rock (Figure 10).

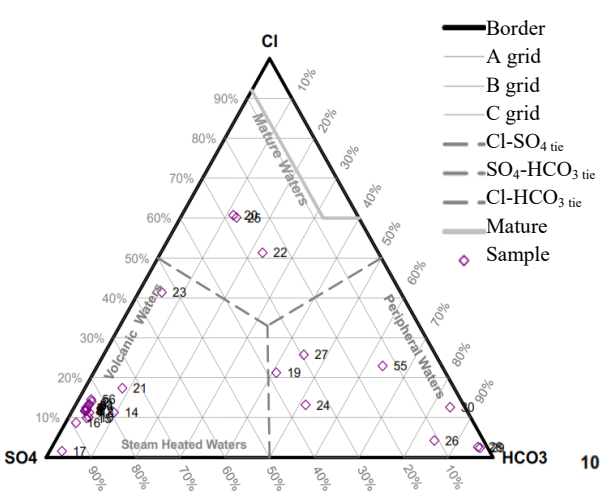


FIGURE 9: Diagram $Cl^{-}$-$SO_4^{-2}$-$HCO_3^{-}$ for San Francisco Libre water samples

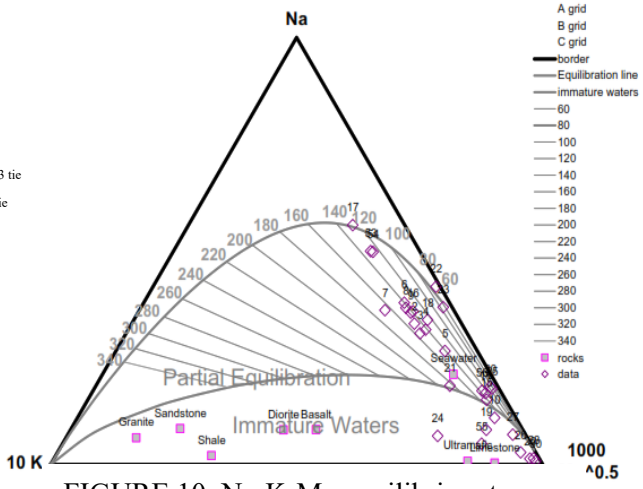


FIGURE 10: Na-K-Mg equilibrium ternary diagram for San Francisco Libre Waters Samples

## 4.2 Geothermometry

Chemical geothermometry calculated for 6 samples (Medical Center, Peña Blanca and sample 025) with the WATCH programme predict temperatures summarised in Table 1.
For the first group of samples (Medical Center - Peña Blanca), the calculated temperatures for the Na/K and chalcedony geothermometers are very similar to the measured values, ranging between 78.1 and 84.8°C. However, the quartz geothermometer gives systematically higher results.
The well sample tells a different story. There the silica geothermometers give temperatures more than 100°C whereas the Na/K geothermometer gives 34°C which is closer to the measured temperature.

TABLE 1: Geothermometer temperatures (°C) calculated with WATCH programme for 6 San Francisco Libre water samples

| Sample | Quartz (Fournier and Potter, 1982) | Chalcedony (Fournier, 1977) | Na/K (Arnórsson et al., 1983) | Na-K-Ca (Fournier and Truesdell, 1973) |
|---|---|---|---|---|
| MC (2013-004) | 115 | 86 | 84 | 57 |
| MC (2013-005) | 114 | 85 | 83 | 50 |
| MC (2013-006) | 115 | 86 | 82 | 50 |
| PB (2013-053) | 107 | 76 | 71 | 66 |
| PB (2013-054) | 104 | 73 | 69 | 42 |
| Well (2013-025) | 143 | 117 | 34 | 228 |

## 4.3 Mineral saturation

The speciation technique was only applied to 6 water samples with the high measured temperatures (> 75°C) or high silica temperatures (>100°C). The minerals adularia, anhydrite, wairakite, albite, calcite, microcline, muscovite, analcime, chalcedony, quartz and zoisite were selected to calculate the equilibrium state (Figure 1 in appendix I). These minerals were chosen for the evaluation of the saturation indices. Due to their content of $SO_4$ and Ca the samples of San Francisco Libre have a high content of calcium and the local geology and various indications of alterations of rocks containing calcite were considered.

Minerals in equilibrium are as follow:

For the first 3 samples located in the medical center the minerals chalcedony, calcite and anhydrite were found in equilibrium (SI=0) at around 80°C and muscovite and quartz were found very close to the equilibrium point at around 100°C. This is again in relatively good agreement with geothermometry and the measured temperatures.
For the samples taken in Peña Blanca the minerals chalcedony and anhydrite were found close to equilibrium at around 80°C and adularia and anhydrate intersect each other at 90°C, again in good agreement with geothermometry and measured temperatures.
For the well sample (number 025) which probably belongs to another system of faults, minerals found in the equilibrium point were microline, analcime and chalcedony intersecting each other at 100-120°C. Here, the mineralogy and silica geothermometry suggest reservoir temperatures exceeding 100°C whereas the Na/K geothermometer suggest a reservoir temperature of 35°C which is more in line with the measured temperature of the hot spring.

## 5. DISCUSSION

The study area suggests two different geothermal systems. The first system is hosted by the fracture system reaching between the Medical center and Peña Blanca. The geochemical composition of these samples indicate that are the same water, they all show similarly low chloride and high temperature. Based on geothermometry (chalcedony and Na/K) and multiple mineral equilibria, the reservoir temperature is around 75-85°C, which is in good agreement with the measured temperature. The very similar composition of those samples suggests that they are most likely coming from the same fault even though they are in different locations.

Indications were found of another geothermal system, for which chalcedony geothermometry and multiple mineral equilibria suggest a temperature around 115°C. On the other hand, Na/K geothermometry suggests a temperature of about 35°C, which is close to the measured temperature. This water clearly belongs to a different water system as the sample has much higher chloride content than the first group of samples. The results strongly indicate the possibility of a system with this temperature, which is an option that should be studied further.

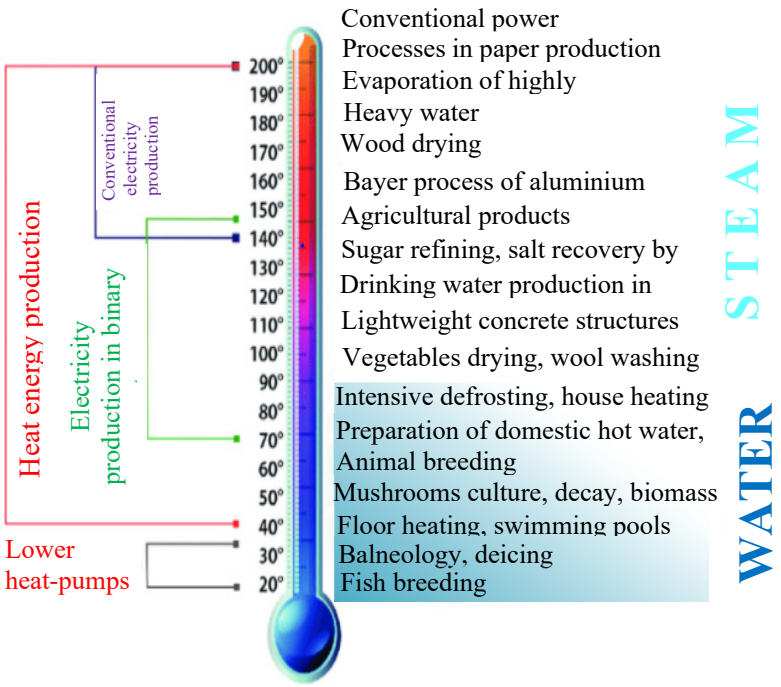


FIGURE 11: Líndal diagram (Guðmundsson et al. 1985

For these two geothermal systems, it is therefore appropriate to look at the Líndal diagram (Figure 11, Guðmundsson et al., 1985) for possible uses of the resources. This water could also be used for cooling buildings or for greenhouses.

When it comes to rehabilitative activities, the temperature in medical pools should be different, 27-28°C is usually

used. If the temperature of the small leisure pools is of concern, it can be raised to 35°C. Temperatures in indoor recreational pools can range from 25 to 35°C, depending on local customs. The temperature of outdoor recreational pools changes depending on the season, being lower in the summer (24-27°C) and higher in the winter (28-35°C). In Japan, they are significantly warmer and sometimes reach 40°C. Finally, temperatures between 25 and 28°C are ideal for both indoor and outdoor swimming pools (Geothermal communities, 2021).

For the second resource it is recommended to collect another sample to confirm the existence of this system. According to the Líndal diagram, it could be possible to use the resource for the development of a binary cycle power generation or several other things.

## 6. CONCLUSIONS

Chemical analyses have been reported for 30 water samples collected from hot springs and wells in San Francisco Libre in 2013. Out of those 30 samples, 6 samples were selected for further geochemical evaluation. The samples have been coded as MC1, MC2, MC3, PB1, PB2 and 025, based on measured temperatures, silica content and salinity.

Two geothermal systems with temperature in the range of 75-85°C and 100-115°C were proposed based on the geothermometry and corroborated by multiple mineral equilibrium plots.

The 75-85°C system (Peña Blanca and Medical Center) is characterized by low salinity and sulfate-dominated water. The measured temperature agrees well with geothermometry.

The 100-115°C system has higher salinity (Cl main anion) and high silica, but the sample temperature is low (30°C). Many forms of direct uses could be applied for this system if it turns out to be as hot as the geothermometry suggests, including a binary cycle power plant.

## ACKNOWLEDGEMENTS

My deepest gratitude to the Government of Iceland for their generosity to support one more time the development of geothermal resources in my country throughout this specialization programme. I also express my deepest gratitude to the Government of Reconciliation and National Union of Nicaragua for their persistent effort to stay leading in geothermal resource development and for supporting me in everything I need. My most profound gratitude goes to all the GRÓ GTP team members for sharing more than academic support but human warmth and sympathy. I am grateful to all the lecturers, especially to Professor Andri Stefánsson who is really inspiring and patient. My deepest gratitude extends to my supervisor, the geochemist Finnbogi Óskarsson, from whom I received the biggest support to complete this program and invaluable knowledge for the future. Also I would like to thank Dr.Vigdís Harðardóttir who always supported me.

And as my dear parents said: “God bless Iceland. God makes everything possible.”

## REFERENCES

Arnórsson, S. (ed.), 2000: *Isotopic and chemical techniques in geothermal exploration, development and use. Sampling methods, data handling, interpretation*. International Atomic Energy Agency, Vienna, 351 pp.

Arnórsson, S., and Bjarnason, J.Ö., 1993: *Icelandic Water Chemistry Group presents the chemical speciation programme WATCH*. Science Institute, University of Iceland, Orkustofnun, Reykjavík, 7 pp.

Arnórsson, S., Gunnlaugsson, E., and Svavarsson, H., 1983: The chemistry of geothermal waters in Iceland II. Mineral equilibria and independent variables controlling water compositions. *Geochim. Cosmochim. Acta*, *47*, 547-566.

Bjarnason, J.Ö., 2010: *The chemical speciation program WATCH, version 2.4*. ÍSOR – Iceland GeoSurvey, Reykjavik, website: *www.geothermal.is/software*

Burke, K., Cooper, J. F., Dewey, P., Mann, P., and Pindell, J. L., 1984: Caribbean tectonic and relative plate motions. In: Boini, W. Hargraves, R. (eds.), *Caribbean South America Plate*. Geological Society of America Mem., New York, 31-63.

ENACAL, 2021: Empresa nicaraguense de Acueductos y Alcantarillados, 2021: *Biblioteca Virtual ENACAL*,website: *www.biblioteca.enacal.com.ni*

Fournier, R.O., 1977: Chemical geothermometers and mixing model for geothermal systems. *Geothermics, 5,* 41-50.

Fournier, R.O., 1991: Water geothermometers applied to geothermal energy. In: D'Amore, F. (coordinator), *Application of Geochemistry in Geothermal Reservoir Development*. UNITAR/UNDP publication, Rome, 37-69.

Fournier, R.O., and Potter, R.W., 1982: An equation correlating the solubility of quartz in water from 25° to 900°C at pressures up to 10,000 bars. *Geochim. Cosmochim Acta, 46*, 1969-1973.

Fournier, R.O., and Truesdell, A.H., 1973: An empirical Na-K-Ca geothermometer for natural waters. *Geochim. Cosmochim. Acta*, *37*, 1255-1275.

Fournier, R.O., White, D.E., and Truesdell, A.H., 1974: Geochemical indicators of subsurface temperature. Part 1, basic assumptions. *U.S. Geol. Survey J. Res, 2*, 259-262.

Geothermal Communities, 2021: *Geothermal Communities*, website: *https://geothermalcommunities.eu/*

Giggenbach, W.F., 1988: Geothermal solute equilibria. Derivation of Na-K-Mg-Ca geoindicators. *Geochim. Cosmochim. Acta, 52*, 2749-2765.

Gíslason, S.R., Heaney, P.J., Oelkers, E.H. and Schott, J. 1997: Kinetic and thermodynamic properties of moganite, a novel silica polymorph. *Geochim. Cosmochim. Acta, 61,* 1193-1204.

Gudmundsson, J.S., Freeston, D.H., and Lienau, P.J., 1985: The Lindal diagram. *Geoth. Res. Council, Transactions, 9,* 15-19.

Kristinsson, S., and Ruíz, J., 2011: *Reconocimiento Geológico del Área de San Francisco Libre*, Ministerio de Energía y Minas, Nicaragua, 23 pp.

Nicholson, K., 1993: *Geothermal fluids: chemistry and exploration techniques*. Springer-Verlag, Berlin, 268 pp.

Pang Z., and Ármannsson, H. (editors), 2006*: Analytical procedures and quality assurance for geothermal water chemistry*. UNU-GTP, Iceland, Report 1, 172 pp.

Powell, T., and Cumming, W., 2010: Spreadsheets for geothermal water and gas geochemistry. *Proceedings of the 35th Workshop on Geothermal Reservoir Engineering, Stanford University, Stanford, CA,* 10 pp.

Seyfried, H., 1991: Depositional sequences and sequence boundary in fore-arc costal embayments. In: McDonald, D.M. (eds.), *Sedimentation, tectonics and eustasy; sea level changes at active margins.* Spec. Pub. Int. Ass. Sed., Oxford, 241-258.

Truesdell, A.H., 1976: Summary of section III - geochemical techniques in exploration. *Proceedings of the 2nd U.N. Symposium on the Development and Use of Geothermal Resources, San Francisco, 1,* liii-lxxix.

White, D.E., 1970: Geochemistry applied to the discovery, evaluation, and exploration of geothermal energy resources. *Geothermics, Sp. issue, 2-1*, 58-80.

## APPENDIX I: Saturation index (log Q/K) vs. temperature calculated

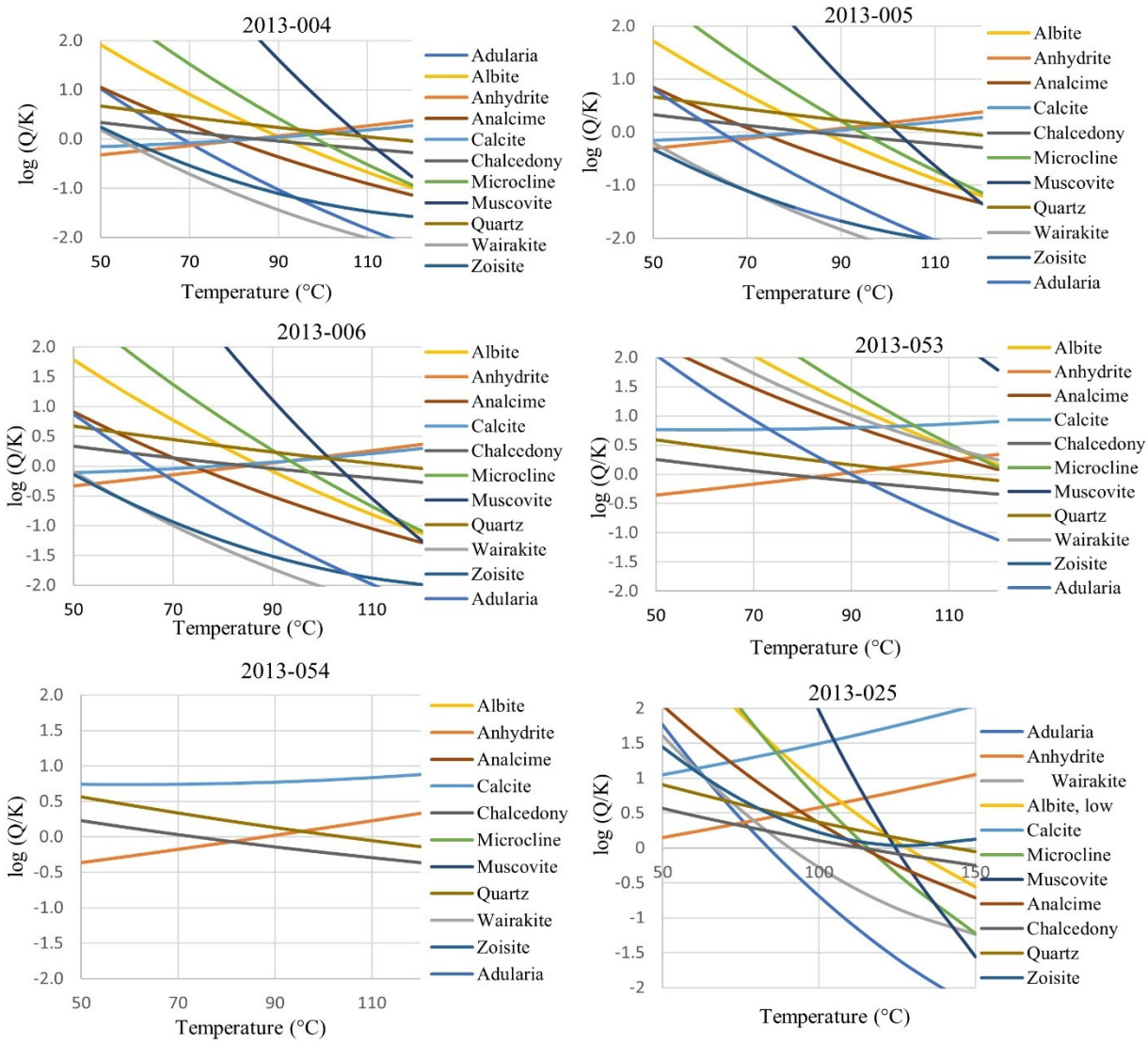


FIGURE 1: Saturation index (log Q/K) vs. temperature calculated with the WATCH program for 6 water samples from the San Francisco Libre area

**APPENDIX II: Tables of results of chemical composition for San Francisco Libre water samples (MEM data base unpublished data)**

| Sample | T | pH | $HCO_3^-$ | $CO_3^{2-}$ | $CO_2$ (Total) | $SiO_2$ | B | Cl | $SO_4$ | Na | Mg | K | Ca | Al | Cu | Fe | Li | Rb | TDS |
|---|---|---|---|---|---|---|---|---|---|---|---|---|---|---|---|---|---|---|---|
| 2013-002 | 34.1 | 8.14 | 27.0 | < 16 | 19.5 | 70.96 | 1.25 | 119.7 | 706.1 | 249.6 | 0.19 | 7.3 | 155.3 | 0.0203 | 0.0052 | 0.03 | < 0.27 | 0.06 | 941 |
| 2013-003 | 38.8 | 8.44 | 28.9 | < 16 | 20.8 | 70.62 | 1.30 | 109.8 | 787.8 | 256.7 | 0.25 | 8.0 | 165.7 | 0.0391 | 0.0059 | < 0.03 | < 0.27 | < 0.05 | 934 |
| MC1 | 84.8 | 8.30 | < 24 | < 16 | 17.3 | 66.81 | 1.14 | 94.8 | 691.7 | 232.7 | 0.20 | 5.9 | 141.3 | 0.0470 | 0.0023 | < 0.03 | < 0.27 | < 0.05 | 852 |
| MC2 | 84.7 | 8.30 | < 24 | < 16 | 17.3 | 65.46 | 1.13 | 99.8 | 714.6 | 232.0 | 0.34 | 5.8 | 142.4 | 0.0311 | < 0.001 | < 0.03 | < 0.27 | < 0.05 | 846 |
| MC3 | 84.7 | 8.38 | < 24 | < 16 | 17.3 | 67.22 | 1.13 | 109.8 | 684.2 | 231.0 | 0.10 | 5.6 | 139.0 | 0.0338 | < 0.001 | < 0.03 | < 0.27 | < 0.05 | 852 |
| 2013-007 | 67.0 | 8.55 | < 24 | < 16 | 17.3 | 68.97 | 1.16 | 109.8 | 748.6 | 239.0 | 0.11 | 9.3 | 147.0 | 0.0414 | < 0.001 | < 0.03 | < 0.27 | < 0.05 | 892 |
| 2013-008 | 72.1 | 8.48 | < 24 | < 16 | 17.3 | 66.25 | 1.18 | 99.8 | 730.4 | 235.0 | 0.12 | 6.1 | 146.0 | 0.0389 | 0.0022 | < 0.03 | < 0.27 | < 0.05 | 868 |
| 2013-009 | 58.0 | 8.44 | < 24 | < 16 | 17.3 | 68.91 | 1.20 | 104.8 | 713.0 | 234.0 | 0.13 | 6.0 | 147.0 | 0.0298 | 0.0025 | < 0.03 | < 0.27 | < 0.05 | 891 |
| 2013-010 | 49.1 | 8.10 | 44.7 | < 16 | 32.2 | 96.26 | 1.33 | 99.8 | 845.8 | 282.0 | 4.77 | 11.2 | 179.0 | 0.0451 | 0.0024 | 0.058 | < 0.27 | < 0.05 | 1065 |
| 2013-011 | 35.5 | 7.28 | 127.2 | < 16 | 91.8 | 73.83 | 0.78 | 64.9 | 524.5 | 180.0 | 1.63 | 6.6 | 129.0 | 0.0198 | 0.0025 | < 0.03 | < 0.27 | 0.05 | 735 |
| 2013-012 | 35.7 | 7.12 | 141.5 | < 16 | 102.1 | 74.46 | 0.98 | 79.8 | 739.5 | 188.0 | 5.46 | 7.3 | 213.0 | 0.0203 | 0.0220 | < 0.03 | < 0.27 | < 0.05 | 905 |
| 2013-018 | 47.2 | 7.81 | 34.1 | < 16 | 24.6 | 68.16 | 1.31 | 94.8 | 713.5 | 261.3 | 0.21 | 5.0 | 125.4 | 0.0135 | 0.0024 | < 0.03 | < 0.27 | < 0.05 | 920 |
| 2013-019 | 30.7 | 7.37 | 273.1 | < 16 | 197.0 | 68.76 | 0.79 | 142.2 | 253.3 | 148.9 | 2.39 | 13.6 | 90.8 | 0.0200 | 0.0019 | 0.052 | < 0.27 | < 0.05 | 626 |
| 2013-020 | 27.9 | 6.74 | 359.4 | < 16 | 259.2 | 113.28 | 0.80 | 1895.7 | 866.0 | 1134.0 | 24.97 | 9.9 | 948.0 | 0.0126 | 0.0060 | 0.054 | < 0.27 | < 0.05 | 4043 |
| 2013-021 | 32.0 | 7.39 | 180.0 | < 16 | 129.8 | 72.31 | 2.35 | 374.1 | 1597.4 | 745.0 | 8.44 | 38.9 | 312.0 | 0.0206 | 0.0130 | < 0.03 | < 0.27 | < 0.05 | 2188 |
| 2013-022 | 25.9 | 7.59 | 885.1 | < 16 | 638.4 | 83.29 | 17.66 | 1995.4 | 1007.1 | 4750.0 | 43.00 | 9.8 | 554.0 | 0.0175 | 0.0420 | < 0.03 | 0.623 | < 0.05 | 9190 |
| 2013-023 | 27.6 | 7.18 | 198.6 | < 16 | 143.3 | 83.4 | 5.24 | 1596.4 | 2058.7 | 1586.0 | 6.97 | 7.8 | 419.0 | 0.0216 | 0.0097 | < 0.03 | 0.257 | < 0.05 | 4115 |
| 2013-024 | 29.1 | 7.75 | 739.2 | < 16 | 533.2 | 96.17 | 1.46 | 189.6 | 507.1 | 286.0 | 10.37 | 77.0 | 180.0 | 0.0278 | 0.0024 | < 0.03 | < 0.27 | < 0.05 | 1232 |
| 2013-025 | 30.1 | 7.14 | 387.3 | < 16 | 279.4 | 113.27 | 0.78 | 1858.3 | 843.2 | 1143.0 | 27.09 | 9.4 | 951.0 | 0.0442 | 0.0062 | 0.049 | < 0.27 | < 0.05 | 4121 |
| 2013-026 | 34.0 | 7.52 | 275.6 | < 16 | 198.8 | 92.98 | 0.08 | 13.9 | 35.7 | 49.1 | 2.62 | 5.3 | 51.0 | 0.0280 | 0.0051 | < 0.03 | < 0.27 | < 0.05 | 228 |
| 2013-027 | 26.9 | 7.69 | 546.2 | < 16 | 394.0 | 62.81 | 1.28 | 314.3 | 359.0 | 428.9 | 30.47 | 15.8 | 87.0 | 0.0196 | 0.0046 | < 0.03 | < 0.27 | < 0.05 | 1252 |
| 2013-028 | 28.6 | 7.24 | 263.8 | < 16 | 190.3 | 98.2 | 0.03 | 7.3 | 5.7 | 34.8 | 5.42 | 2.7 | 39.3 | 0.0261 | 0.0016 | < 0.03 | < 0.27 | < 0.05 | 197 |
| 2013-029 | 29.9 | 7.36 | 261.9 | < 16 | 188.9 | 93.48 | 0.03 | 6.7 | 4.6 | 37.8 | 7.02 | 5.3 | 32.0 | 0.0378 | 0.0061 | 0.143 | < 0.27 | < 0.05 | 190 |
| 2013-030 | 28.1 | 7.13 | 217.2 | < 16 | 156.7 | 80.04 | 0.03 | 32.6 | 8.6 | 30.8 | 15.04 | 4.3 | 35.0 | 0.0366 | < 0.001 | < 0.03 | < 0.27 | < 0.05 | 219 |
| 2013-031 | 29.1 | 7.23 | 261.9 | < 16 | 188.9 | 96.58 | 0.04 | 16.0 | 6.8 | 44.0 | 9.44 | 4.1 | 32.0 | 0.0227 | 0.0023 | < 0.03 | < 0.27 | < 0.05 | 213 |
| PB1 | 78.1 | 8.34 | < 24 | < 16 | 17.3 | 63.6 | 1.13 | 107.5 | 684.8 | 212.3 | 0.03 | 4.2 | 131.3 | - | - | < 0.03 | < 0.27 | 0.07 | - |
| PB2 | 79.0 | 8.45 | < 24 | < 16 | 17.3 | 59.53 | 1.11 | 107.5 | 683.6 | 208.8 | 0.03 | 4.0 | 128.0 | - | - | < 0.03 | < 0.27 | 0.07 | - |
| 2013-055 | 24.5 | 9.12 | 437.3 | < 16 | 315.4 | 7.62 | 1.42 | 157.5 | 90.6 | 217.2 | 14.43 | 44.6 | 27.9 | - | - | < 0.03 | < 0.27 | 0.07 | - |
| 2013-056 | 71.1 | 8.57 | < 24 | < 16 | 17.3 | 67.26 | 1.16 | 125.0 | 710.6 | 252.4 | 1.34 | 5.4 | 144.2 | - | - | 0.038 | < 0.27 | 0.07 | - |